



ELSEVIER

Physica A 295 (2001) 17–30

PHYSICA A

www.elsevier.com/locate/physa

Physics of the cigarette filter: fluid flow through structures with randomly-placed obstacles

H. Eugene Stanley^{a,*}, José S. Andrade Jr.^b

^aCenter for Polymer Studies and Department of Physics Boston University, Boston, MA 02215, USA

^bDepartamento de Física, Universidade Federal do Ceará, 60451-970 Fortaleza, Ceará, Brazil

Abstract

This talk briefly reviews the subject of fluid flow through disordered media. In particular, we focus on the sorts of considerations that may be necessary to move statistical physics from the description of idealized flows in the limit of zero Reynolds number to more realistic flows of real fluids moving at a nonzero velocity, where inertia effects mean that dangling ends are explored and the backbone is not entirely explored by the fluid. We discuss several intriguing features, such as the surprisingly sharp change in behavior from a localized to delocalized flow structure (distribution of flow velocities) that seems to occur at a critical value of Re which is orders of magnitude smaller than the critical value of Re where turbulence sets in. © 2001 Published by Elsevier Science B.V.

Keywords: Percolation; Turbulence; Respiration; Wetting

1. Introduction

1.1. What is the scientific question associated with fluid flow through disordered structures?

The primary question for physicists to entertain is: what happens to the “laws of fluid flow” when the medium through which the fluid actually flows is disordered? What happens when the particles of the fluid are not passing through a medium that resembles a straight pipe, but one that is full of disorder, e.g., the filter of a cigarette?

* Corresponding author. Tel.: +1-617-3532617; fax: +1-617-3533783.
E-mail address: hes@bu.edu (H.E. Stanley).

1.2. Why do we care about this question?

The scientific reason for our interest in this topic is immediately obvious: the laws associated with fluid flow through disordered media are only beginning to be understood [1–4]. There is much interesting work to be done before a complete understanding is obtained.

The practical reasons for our interest are numerous:

- The oil in the earth is not contained in some kind of a “balloon”, released when the balloon is punctured—the time of gushing oil wells in Oklahoma has long since passed. Rather, two-thirds of the world’s oil supply is held in porous earth—much the same way as water is held in a sponge. We can squeeze a sponge to release the water, but cannot perform an analogous action on a portion of porous earth to release the oil. One technique that is being used to force oil out of the ground involves drilling a second well some distance away (e.g., 1 km) from the original well and pumping some other fluid, such as water, into this second well. Because the earth is porous, the fluid from this second well can often “push” the oil through the ground, and out of the first well. As we might expect, oil companies are very interested in the numerous laws of physics associated with this flow of oil and fluid [5,6]. They want to know, among other things, how to calculate the time of breakthrough, i.e., they want to know the amount of time it takes the injected fluid to push the oil out. In order to calculate that time, they need to know the path the oil takes in this very disordered sponge called the earth.
- Fluid flow in branching geometries is related to many phenomena in physics, geology and biology. Examples range from fluid flow through porous media [4,7] to respiration [8] and blood circulation [9]. In particular, the mechanism of flow bifurcation plays a crucial role in the functioning of the respiratory and circulatory systems. Air does not enter a lung the way air fills a balloon, but enters a ramified, tree-like structure with approximately 20 generations or 2^{20} branches. As the stream of air enters, it bifurcates at each of these branches. This bifurcation is not symmetric, and different parts of the lung can exhibit very different levels of aeration. The lung is also a disordered medium. Diseases such as emphysema can introduce disorder into this system of asymmetrical branches by partially blocking some of the airways. How this kind of disorder affects lung functioning is another problem for physicists.
- Because cigarette smoke contributes so significantly to lung cancer, cigarette manufacturers are extremely interested in the physical laws associated with smoke passing through the disordered medium of the cigarette filter. Indeed, it may be time that they begin to invest in research relevant to the discovery of these laws.

There are many other examples of practical interest we might have in the laws associated with fluid flow through disordered media.

1.3. *What do we actually do in pursuing this question?*

As physicists, our approach to problems is to discover what we can quantify. But what can we quantify when the subject is, by definition, disordered? It is not perfectly obvious what we are going to be able to quantify in a cigarette filter.

If we have no randomness in the flow path of a fluid, we know how to treat the situation. But if we start placing obstacles in the flow path, everything becomes much more complex. Work on percolation models has shown us that the actual positioning of the obstacles is extremely important. Placing them in a completely uncorrelated pattern is a simple first step, and it corresponds to an idealized limit. But almost nothing is really uncorrelated. If we have inclusion zones in porous earth, their presence is not uncorrelated. If we have a permeability in zone k_1 , then the permeability zone k_2 has something to do with k_1 —its permeability is not simply random. There is a correlation in the spatial disorder.

We should take special note of the fact that almost nothing has been done in the area of correlated percolation with some notable exceptions. For example, Coniglio [10] has noted that correlated disorder is an important form of disorder (e.g., in the growth of cities [11,12]), and random multiplicative correlations have also been studied [13,14].

So most disorders, most obstacles in the flow path of a fluid, are placed in an uncorrelated fashion—somewhat like the potholes in the streets of my home city, Boston. And like Boston potholes, uncorrelated obstacles can often stop the flow completely, and not just impede it.

2. **Idealized model for the limit of zero inertia**

There are many ways of generating percolation. One of the easiest and most useful to us is the algorithm that produces invasion percolation [15,1,2]. This algorithm drives the system until it reaches the critical point.

In this algorithm, we “wet” one square pixel near the center of the computer screen, and randomly generate numbers for the four neighboring pixels having replaced the continuum by a lattice [16,17]. The “fluid” then randomly “wets” the pixel with the lowest random number, and a tiny percolation cluster of size 2 is the result. The newly-wetted site is surrounded by three fresh sites. The random numbers are generated for these three sites, the site with the lowest random number is wetted, and the percolation cluster is now size 3. This algorithm is iterated until a large cluster emerges. If we make a histogram of the random numbers associated with the occupied sites, the curve is flat until we reach a critical value, the percolation threshold p_c , at which time it plunges almost to zero. The width of that transition region scales as a power law with system size, i.e., the reciprocal of the system size to some critical exponent—the critical exponent of the singly-connected “red” bonds [18,19].

If we examine our percolation cluster visually, and on several scales (use two vertical and two horizontal lines to divide the screen into nine equal squares and magnify the middle square until it is as big as the screen—repeat as desired), we notice that the texture of the cluster seems to be the same, irrespective of the scale. It is difficult to distinguish the original screen-filling cluster from the magnified portion of that original—and a magnified portion of that magnified portion (see Figs. 1 and 2 of Ref. [20]).

This shows that this simple algorithm of wetting neighboring sites on a computer screen generates a fractal structure, i.e., one that is self-similar. Each part of the original is similar to the whole. Indeed, percolation (unlike some of the natural systems discussed in Refs. [21] and [22]) is a true fractal. The total number of wet sites inside a box as a function of L (the edge of the box) will be some number less than two. This number is called the fractal dimension, which has been solved exactly as 1.89 in two-dimensional percolation [15,1]. The behavior of this fractal dimension in the nonclassical region and below the critical dimension is an unsolved problem. Work can be done using approximations, e.g., brute force computer simulations or position-space renormalization group (PSRG).

In PSRG, we take a 2×2 Kadanoff cell in which each site exists with probability p . We map this 2×2 group into a cell that will be wetted with probability p' . The goal in this PSRG is to find the expression that relates this wetting probability p' of the cell to the initially wetting probability p of the underlying lattice. In this 2×2 case, when all four cells are occupied there is a connecting path from bottom to top (“south to north”)—remembering that we want to get oil out of the ground—and when there are three cells occupied there is still a connected south-to-north path. If we have only two occupied, two of the six possible configurations still provide a connected south-to-north path.

This procedure is not very accurate for 2×2 cells, but by using a combination of Monte Carlo methods and renormalization group concepts, one can consider a sequence of cells, starting with two and going up to one thousand. That sequence of larger and large cells has so many configurations (2^{L^2}) that it is impossible to work out, but by using sampling procedures one can get an approximate recursion relation [23,24].

How does a fluid go through a medium when there are obstacles in water? The structure of the cluster at the exact moment it connects the percolation threshold—the *incipient* infinite cluster (i.i.c.)—is sometimes called the wetting path or the backbone. Notice that there are dangling ends in this structure. If we inject a current into this idealized structure, then these dead ends are not going to connect to anything. What happens if we throw them away? The first thing to notice is that we no longer have a fractal of dimension 1.89! If what we threw away was a fixed fraction independent of size (e.g., 90 per cent of the total cluster), then the fractal dimension would not be changed. But this is not the case, because these dead ends are such an overwhelmingly large fraction of the total cluster that when we do throw them away, we reduce the fractal dimension of the cluster. The fractal dimension of the cluster without its dead ends—i.e., the fractal dimensions of just the wetting path—is roughly 1.62 [25,26].

In this wetting path, we distinguish between two different kinds of bonds: “blobs”, which have multiple connections (a variety of routes within the wetting path), and singly-connected bonds (“red bonds”), which must carry 100 per cent of the fluid traversing the wetting path [18,19]. The structure of the wetting path is, therefore, a kind of necklace of blobs and single-connection bonds. Both the blobs and red bonds are themselves fractals with self-similarity.

3. Minimum wetting path

The minimum path is a subset of the total wetting path, characterized not by the amount of fluid that flows through it, but by the question of what is the shortest path distance ℓ between two points in this model random medium. The length of this minimum path does not increase linearly as the straight-line distance between the beginning and ending of the total wetting path is increased. The longer the total straight-line distance, the more likely the significant obstacles will be encountered and the total minimum path lengthened (Fig. 1). The function that describes this increase is once again a fractal object with an exponent d_{\min} , an exponent for which an exact result has not yet been found, even for dimension $d = 2$ [27,28].

In real-world problems, such as drilling oil wells, one does not “average over a million realizations”. There is a given oil field, and that is it. Simple “appropriate averages” have no bearing on the situation. In a real oil field, we care about the entire distribution of shortest paths. The function of interest to us is the conditional probability $P(\ell|r)$ for two sites to be separated by the shortest path ℓ , given that the geometrical distance between these sites is r

At the percolation threshold, it has been shown [29,30] that

$$P(\ell|r) \sim \frac{1}{r^{d_{\min}}} \left(\frac{\ell}{r^{d_{\min}}} \right)^{-g_{\ell}} \exp \left(-a \left(\frac{\ell}{r^{d_{\min}}} \right)^{-\phi_{\ell}} \right). \quad (1)$$

The probability distribution of more practical interest is $P'(\ell|r)$, defined in the same way as $P(\ell|r)$ but for any two randomly chosen points separated by geometrical distance r and on the same cluster, but not necessarily on the incipient infinite cluster [29,30]. $P'(\ell|r)$ has the same scaling form as in Eq. (1), but with g_{ℓ} replaced by [29,30]

$$g'_{\ell} = g_{\ell} + \frac{d - d_f}{d_{\min}}. \quad (2)$$

The complete scaling form of $P'(\ell|r)$, which accounts also for finite size effects and off-critical behavior, has been studied for $d = 2$ and reported in Refs. [29,30]. Specifically, the following *Ansatz* has been proposed [29,30]

$$P'(\ell|r) \sim \frac{1}{r^{d_{\min}}} \left(\frac{\ell}{r^{d_{\min}}} \right)^{-g'_{\ell}} f_1 \left(\frac{\ell}{r^{d_{\min}}} \right) f_2 \left(\frac{\ell}{L^{d_{\min}}} \right) f_3 \left(\frac{\ell}{\xi^{d_{\min}}} \right), \quad (3)$$

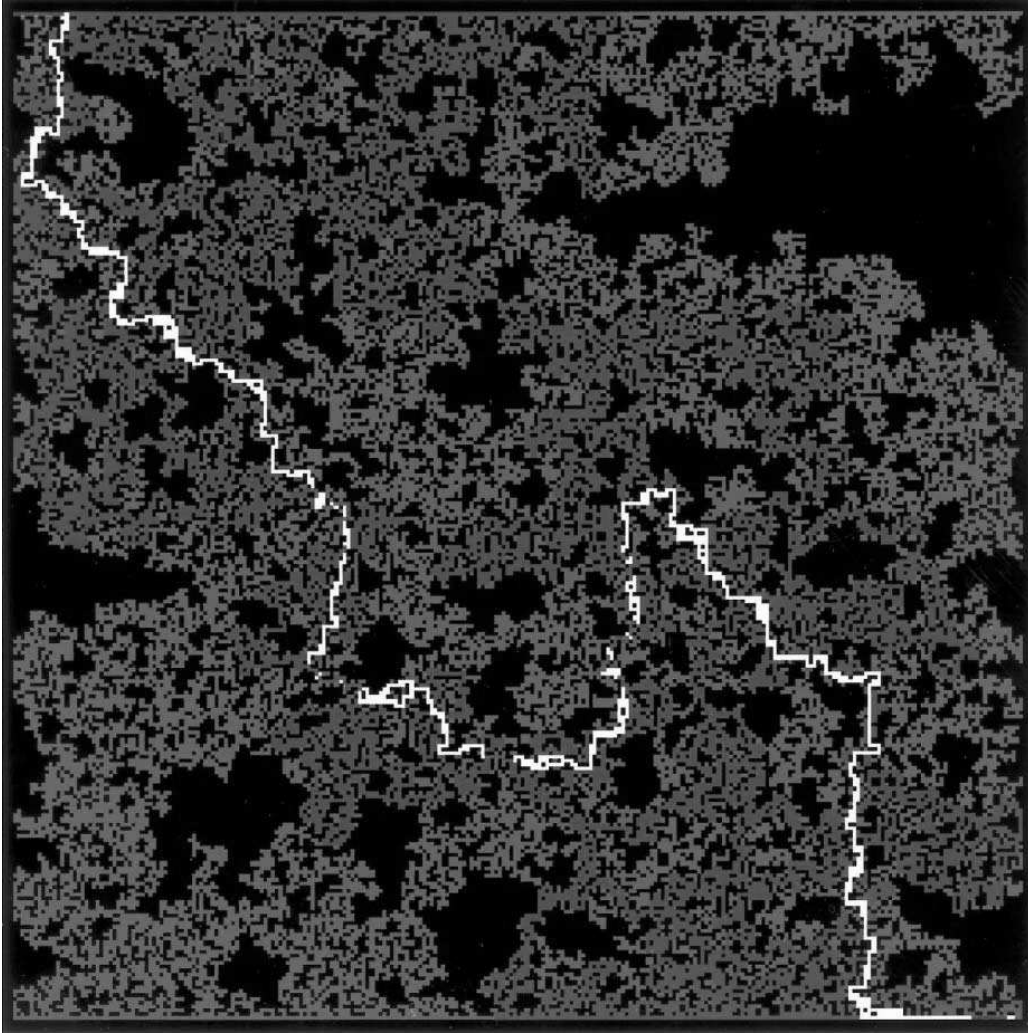


Fig. 1. The incipient infinite percolation cluster that forms at the percolation threshold, highlighting the path that connects one point to another using the minimum number of bonds. This “minimum path” is a fractal object whose dimension is not known exactly even for the case of a two-dimensional cluster (but is approximately 1.13). The average chemical distance scales with exponent d_{\min} , where various estimates of d_{\min} are $d_{\min} \approx 1.130 \pm 0.005$ [28] and $d_{\min} \approx 1.1307 \pm 0.0004$ [25] (courtesy of S. Schwarzer).

where $\xi \sim |p - p_c|^{-\nu}$ is the pair connectedness length, and the scaling functions have the form

$$f_1(x) \equiv \exp(-ax^{-\phi}), \quad f_2(x) \equiv \exp(-bx^\psi), \quad \text{and} \quad f_3(x) \equiv \exp(-cx). \quad (4)$$

The function f_1 accounts for the lower cut-off due to the constraint $\ell > r$, while f_2 and f_3 account for the upper cut-offs due to the finite size effect and due to the finite correlation length, respectively. Either f_2 or f_3 becomes irrelevant, depending on the magnitudes of L and ξ : for $L < \xi$, f_2 dominates the upper cut-off, otherwise f_3 dominates. We assume the independence of the finite size effect and the effect of the concentration of the occupied sites, so that Eq. (3) can be represented as a product

of the terms which are responsible for the finite size effect (f_2) and the effect of the concentration (f_3). Simulations have been performed in Refs. [29–32] and support this assumption.

Finally, it is worth mentioning that only a few studies have been devoted to the investigation of the displacement process of a viscous fluid by a less viscous one through percolation porous media. Murat and Aharony [33] showed by numerical simulation of two-dimensional diluted percolation lattices that, although the clusters generated from viscous fingering and diffusion limited aggregation have the same fractal dimension at the vicinity of the critical point, many other geometrical differences can be observed between these two processes. In two recent studies [31,32], the dynamics of viscous displacement through percolation porous media has been investigated in the limiting condition of unitary viscosity ratio, $m \equiv \mu_2/\mu_1 = 1$, where μ_1 and μ_2 are the viscosities of the injected and displaced fluids, respectively. In this situation, the displacement front can be approximately modeled by tracer particles that follow the streamlines of the flow. As a result, it was shown that the distributions of shortest path and minimal traveling time of the tracer closely obey the scaling *Ansatz* Eq. (1). More recently [34], it was found by numerical simulations on $2d$ percolation networks at criticality that the scaling *Ansatz* (1) also holds for the case of very large viscosity ratio, $m \rightarrow \infty$. Surprisingly, it was shown that the distribution exponents estimated for the two limiting cases $m=1$ and $m \rightarrow \infty$ are statistically identical. Based on this fact, it was suggested that the two processes belong to the same universality class.

4. Flow of fluids with inertia

When we are talking about a realistic fluid flow, we are not talking about something that behaves necessarily like an electrical current. Fluid flow can have inertia; if it is too fast, it “plows ahead” like a crowd in a railway station. When a slow-moving fluid tries to make a turn in, e.g., a “bent pipe”, it is able to make the turn in a more-or-less smooth fashion; since the fluid is laminar (Fig. 2), the velocity of the fluid varies smoothly across the cross section of the bent pipe, being zero on the walls. If the Reynolds number is higher, the fluid does not make the turn in the same way, and a lot of inertial activity results (Fig. 3).

These features of the fluid flow phenomenon in irregular geometries have not been intensively studied before, at least from a microdynamical perspective. In order to investigate them, it is necessary to perform direct simulations of the Navier–Stokes equations at the scale of the pore [35–37]. We adopt the general picture of site percolation disorder as a simplified model for pore connectivity. Square obstacles are randomly removed from a 64×64 square lattice until a porous space with a prescribed void fraction ε is generated. The mathematical description for the detailed fluid mechanics in the interstitial pore space is based on the assumptions that we have steady state flow in isothermal conditions and the fluid is continuum, Newtonian and

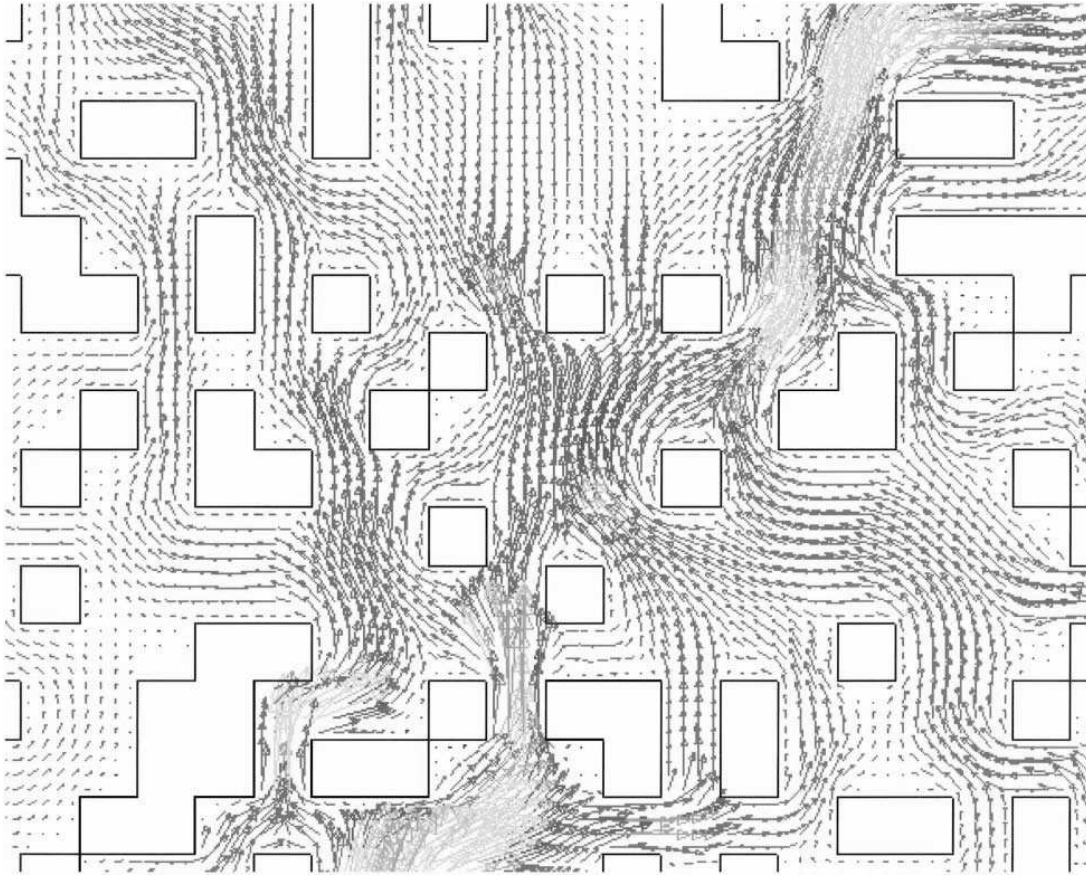


Fig. 2. Subset of the velocity vector field taken from a realization of the porous media generated with $\varepsilon=0.7$ at $Re = 0.0156$. Each vector represents the magnitude and direction of the local velocity. Fluid is pushed from bottom to top in the pore network.

incompressible. We use the nonslip boundary condition at the whole of the solid–fluid interface. End effects of the flow field established inside the pore structure are minimized by attaching an inlet and an outlet to two opposite faces. At the inlet, a constant inflow velocity in the normal direction to the boundary is specified, whereas at the outlet the rate of velocity change is assumed to be zero (gradientless boundary condition). The Reynolds number

$$Re \equiv \frac{\rho d_p \bar{v}}{\mu} \quad (5)$$

characterizes the relative contributions from convective and viscous mechanisms of momentum transfer in fluid flow, where ρ is the density, d_p the particle size, μ the kinematic viscosity and \bar{v} the average fluid velocity. For a given realization of the pore geometry and a fixed Re , the local velocity and pressure fields in the fluid phase of the void space, head and recovery zones are numerically obtained through discretization by means of the control volume finite-difference technique [38]. We discretize the governing balance equations within the pore space domain using square grid elements

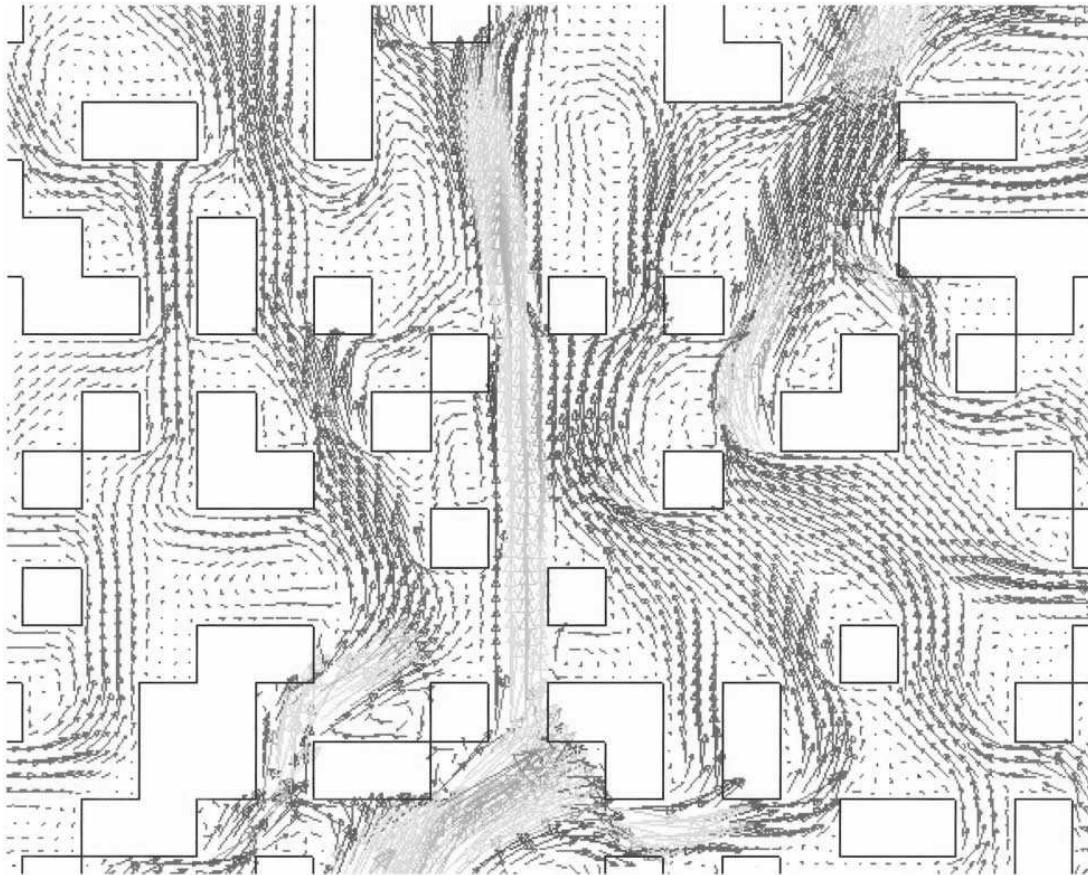


Fig. 3. Same as Fig. 2, but now for a Reynolds number 1000 times larger ($Re=15.6$). The complex structure of the porous system creates very tortuous pathways for fluid flow. The effect of inertia is revealed by the significant redistribution of the fluid flow in the pore space and the presence of several vortices and zones of “flow separation”.

with length equal to one-quarter of the solid cell size, $d_p/4$. In other words, while the physical system comprises 64×64 elements (solid or fluid cells of size d_p), the corresponding numerical mesh has 256×256 discretization cells.

First, we study fluid flow under conditions of low Reynolds number to ensure that the contribution from inertial terms (convection) does not prevail over the viscous mechanism of momentum transfer. In spite of the well-connected pathways available for flow at a large porosity value, the predominant viscous forces in the momentum transport through the complex void geometry generates well defined “hot spots” of fluid flow (see Fig. 4). As shown in Fig. 5, the situation is somewhat different at higher Reynolds conditions. Due to the relevant contribution of inertial forces (convection) to the transport at the pore scale, the flow distribution along the direction orthogonal to the main flux becomes more uniform.

At lower porosities [39,35], another result of inertia is that the fluid activity can “fill” the dead ends of the system and also that it does not need to “fill” the entire backbone

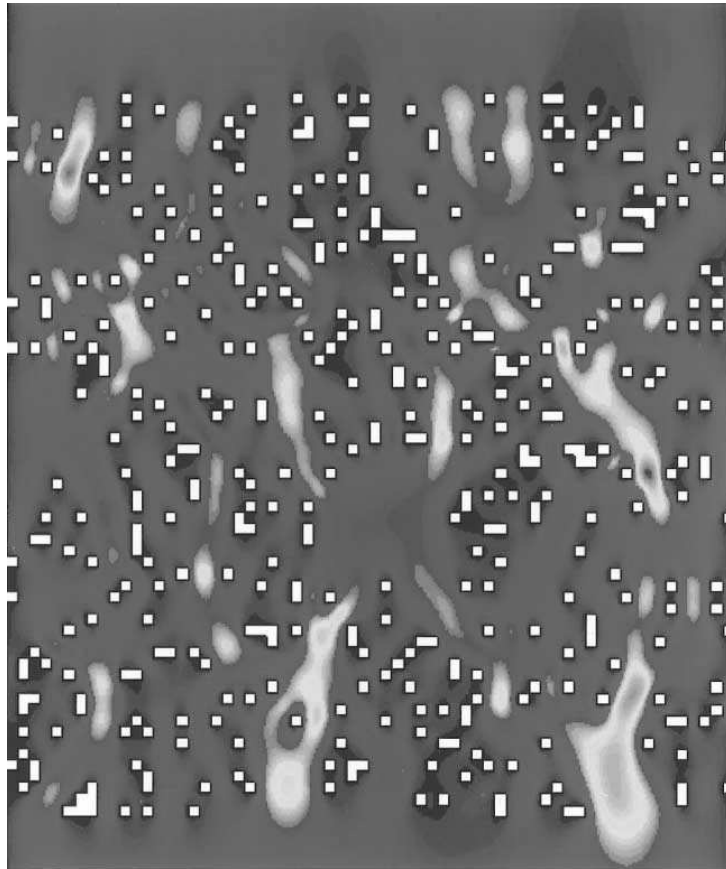


Fig. 4. Flow in disordered porous media. We show the contour plot of the velocity magnitude for a typical realization of a highly porous void space ($\varepsilon = 0.9$) subjected to low Reynolds conditions, $Re = 0.0156$. The colors ranging from blue to red correspond to low and high velocity magnitudes. Notice that the flow is “spatially” localized.

(see Figs. 2 and 3). The procedure of throwing away dead ends now becomes suspect. Also, the fluid is not very smart. There are backwaters and eddies and countercurrents set up as the fluid makes its way from south to north. We can see features in this porous system that look like turbulence without the system itself being turbulent. The Reynolds number in Fig. 3 is about 15 and the onset of turbulence does not occur until a Reynolds number is about 35.

The “localization” effect shown in Fig. 4 can be statistically quantified in terms of the spatial distribution of kinetic energy in the flowing system. In analogy with previous work on localization of vibrational modes in harmonic chains [40], we define a “participation” number π ,

$$\pi \equiv \left(n \sum_{i=1}^n q_i^2 \right)^{-1} \quad \left(\frac{1}{n} \leq \pi \leq 1 \right), \quad (6)$$

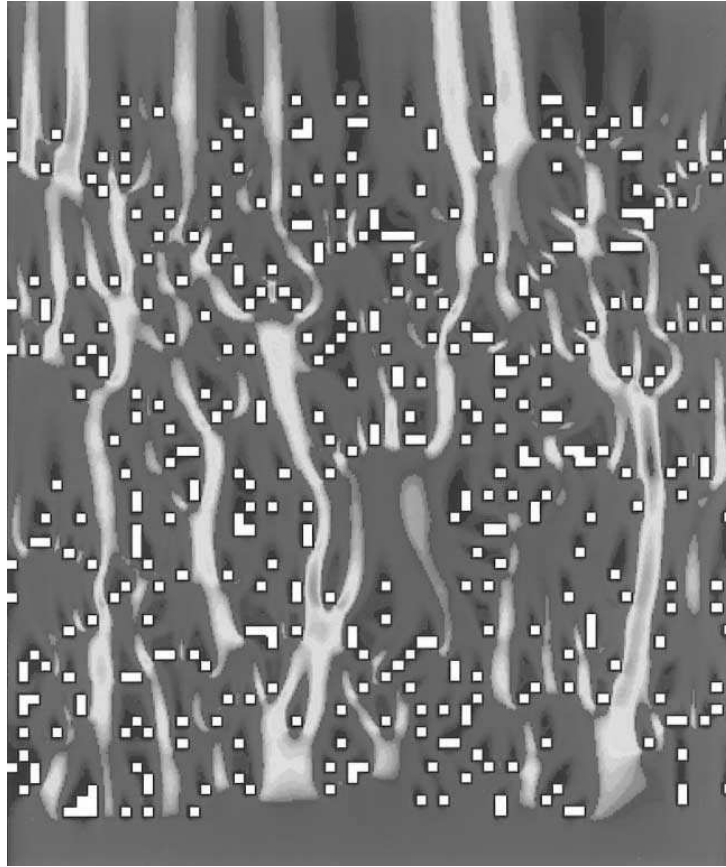


Fig. 5. Same as Fig. 4, but for a Reynolds number 1000 times larger ($Re = 15.6$). Notice that compared to Fig. 4 the flow is now spatially “delocalized”.

where n is the total number of fluid cells in the numerical grid enclosing the physical pore space,

$$q_i \equiv \frac{e_i}{\sum_{j=1}^n e_j}, \quad (7)$$

where $e_i \propto (u_i^2 + v_i^2)$ is the kinetic energy associated with each individual fluid cell, and u_i and v_i are the components of the velocity vector at cell i in the x and y directions, respectively. From the definition, Eq. (6), $\pi = 1$ indicates a limiting state of equal partition of kinetic energy ($q_i = 1/n$, $\forall i$). On the other hand, a sufficiently large system ($n \rightarrow \infty$) should correspond to a “localized” flow field, $\pi \approx 0$. The function π has been calculated for 10 pore space realizations generated with a porosity $\varepsilon = 0.9$. As shown in Fig. 6, the participation number remains constant, $\pi \approx 0.37$, for low Re up to a transition point at about $Re \approx 0.3$. Above this point, the flow becomes gradually less “localized” (π increases) as Re increases. This transition reflects the onset of convective effects in the flow, and the significant changes in π above the transition point indicate the sensitivity of the system to these nonlinearities. The large error bars at low Reynolds conditions indicate that π is sensitive to structural disorder if the viscous forces are effectively generating preferential channels in the flow.

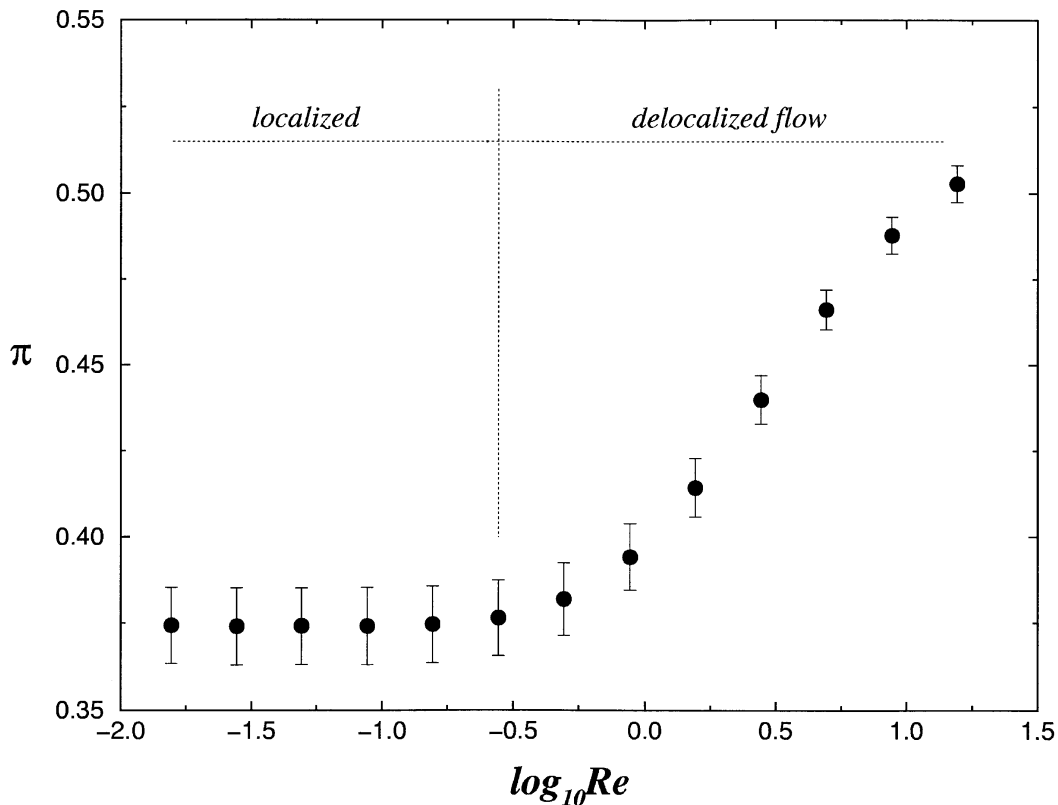


Fig. 6. Dependence of the participation number π on the Reynolds number, Re ($\varepsilon = 0.9$). These simulations have been performed with ten lattice realizations. We find a relatively sharp change in behavior from a localized (small π) to delocalized (larger π) at a critical value of Re , whose size is an order of magnitude smaller than the value of Re for the onset of turbulence.

Acknowledgements

We thank our co-authors whose work is reported here, particularly M.P. Almeida, A.D. Araújo, S.V. Buldyrev, F.S.A. Cavalcante, U.M.S. Costa, N.V. Dokholyan, S. Havlin, P.R. King, Y. Lee, H.A. Makse, G. Paul, and B. Suki. We also thank BP, CNPq, FUNCAP and NSF for financial support.

References

- [1] D. Ben-Avraham, S. Havlin, Diffusion and Reactions in Fractals and Disordered Systems, Cambridge University Press, Cambridge, 2000.
- [2] A. Bunde, S. Havlin (Eds.), in: Fractals and Disordered Systems, Springer, New York, 1996.
- [3] M. Sahimi, Flow phenomena in rocks: from continuum models to fractals, percolation, cellular-automata, and simulated annealing, Rev. Mod. Phys. 65 (1993) 1393.
- [4] M. Sahimi, Applications of Percolation Theory, Taylor & Francis, London, 1994.
- [5] P.R. King, J. Andrade, N.V. Dokholyan, S.V. Buldyrev, S. Havlin, Y. Lee, H.E. Stanley, Percolation and oil recovery, Physica A 266 (1999) 107–114.

- [6] P.R. King, S.V. Buldyrev, N.V. Dokholyan, S. Havlin, Y. Lee, G. Paul, H.E. Stanley, Applications of statistical physics to the oil industry: predicting oil recovery using percolation theory, *Physica A* 274 (1999) 60–66.
- [7] P.M. Adler, *Porous Media: Geometry and Transport*, Butterworth-Heinemann, Stoneham, MA, 1992.
- [8] R.H. Ingram Jr., T.J. Pedley, in: *Handbook of Physiology. The Respiratory System. Mechanics of Breathing*, American Physiological Society, Bethesda, 1986.
- [9] D. MacDonald, *Blood Flow in Arteries*, Williams & Wilkins, Baltimore, 1974.
- [10] A. Coniglio, C. Nappi, L. Russo, F. Peruggi, Percolation points and critical point in the Ising model, *J. Phys. A* 10 (1977) 205.
- [11] H. Makse, S. Havlin, H.E. Stanley, Modeling urban growth patterns, *Nature* 377 (1995) 608.
- [12] H.A. Makse, J.S. Andrade, M. Batty, S. Havlin, H.E. Stanley, Modeling urban growth patterns with correlated percolation, *Phys. Rev. E* 58 (1998) 7054.
- [13] S. Havlin, R. Selinger, M. Schwartz, H.E. Stanley, A. Bunde, Random multiplicative processes and transport in structures with correlated spatial disorder, *Phys. Rev. Lett.* 61 (1988) 1438.
- [14] S. Havlin, M. Schwartz, R. Blumberg Selinger, A. Bunde, H.E. Stanley, Universality classes for diffusion in the presence of correlated spatial disorder, *Phys. Rev. A* 40 (1989) 1717.
- [15] D. Stauffer, A. Aharony, *Introduction to Percolation Theory*, Taylor & Francis, Philadelphia, 1994.
- [16] A. Geiger, H.E. Stanley, Tests of universality of percolation exponents for a 3-dimensional continuum system of interacting waterlike particles, *Phys. Rev. Lett.* 49 (1982) 1895.
- [17] E.T. Gawlinski, H.E. Stanley, Continuum percolation in two dimensions: Monte Carlo tests of scaling and universality for non-interacting discs, *J. Phys. A* 14 (1981) L291.
- [18] H.E. Stanley, Cluster shapes at the percolation threshold: an effective cluster dimensionality and its connection with critical-point exponents, *J. Phys. A* 10 (1977) L211.
- [19] A. Coniglio, Thermal phase transition of the dilute s -state potts and n -vector models at the percolation threshold, *Phys. Rev. Lett.* 46 (1981) 250.
- [20] H.E. Stanley, J.S. Andrade Jr., S. Havlin, H.A. Makse, B. Suki, Percolation phenomena: a broad-brush introduction with some recent applications to porous media, liquid water, and city growth, *Physica A* 266 (1999) 5–16.
- [21] D. Avnir, O. Biham, D. Lidar, O. Malcai, Is the geometry of nature fractal? *Science* 279 (1998) 39–40.
- [22] O. Malcai, D.A. Lidar, O. Biham, D. Avnir, Scaling range and cutoffs in empirical fractals, *Phys. Rev. E* 56 (1997) 2817–2828.
- [23] P.J. Reynolds, H.E. Stanley, W. Klein, A large-cell Monte Carlo renormalization group for percolation, *Phys. Rev. B* 21 (1980) 1223–1245.
- [24] H.E. Stanley, Scaling, universality, and fixed points: three pillars of modern critical phenomena, *Rev. Mod. Phys.* 71 (1999) S358–S366.
- [25] P. Grassberger, Conductivity exponent and backbone dimension in 2-d percolation, *Physica A* 262 (1999) 251.
- [26] H.J. Herrmann, H.E. Stanley, Building blocks of percolation clusters: volatile fractals, *Phys. Rev. Lett.* 53 (1984) 1121–1124.
- [27] R. Pike, H.E. Stanley, Order propagation near the percolation threshold, *J. Phys. A* 14 (1981) L169.
- [28] H.J. Herrmann, H.E. Stanley, The fractal dimension of the minimum path in two- and three-dimensional percolation, *J. Phys. A: Math. Gen.* 21 (1988) L829.
- [29] N.V. Dokholyan, Y. Lee, S.V. Buldyrev, S. Havlin, P.R. King, H.E. Stanley, Scaling of the distribution of shortest paths in percolation, *J. Stat. Phys.* 93 (1998) 603–613.
- [30] N.V. Dokholyan, S.V. Buldyrev, S. Havlin, P.R. King, Y. Lee, H.E. Stanley, Distribution of shortest paths in percolation, *Physica A* 266 (1999) 55–61.
- [31] Y. Lee, J.S. Andrade Jr., S.V. Buldyrev, N. Dokholyan, S. Havlin, P.R. King, G. Paul, H.E. Stanley, Traveling time and traveling length for flow in porous media, *Phys. Rev. E* 60 (1999) 3425.
- [32] J.S. Andrade, S.V. Buldyrev, N.V. Dokholyan, S. Havlin, P.R. King, Y.K. Lee, G. Paul, H.E. Stanley, Flow between two sites on a percolation cluster, *Phys. Rev. E* 62 (2000) 8270–8281.
- [33] M. Murat, A. Aharony, Viscous Fingering and Diffusion Limited Aggregates near Percolation, *Phys. Rev. Lett.* 57 (1986) 1875.
- [34] J.S. Andrade Jr., A.D. Araújo, S.V. Buldyrev, S. Havlin, H.E. Stanley, The dynamics of viscous penetration in percolation porous media, *Phys. Rev. E* 63 (2001).
- [35] J.S. Andrade Jr., M.P. Almeida, J. Mendes Filho, S. Havlin, B. Suki, H.E. Stanley, Fluid flow through porous media: the role of stagnant zones, *Phys. Rev. Lett.* 79 (1997) 3901.

- [36] J.S. Andrade Jr., U.M.S. Costa, M.P. Almeida, H.A. Makse, H.E. Stanley, Inertial effects on fluid flow through porous media in disordered porous media, *Phys. Rev. Lett.* 82 (1999) 5249–5252.
- [37] H. Makse, J.S. Andrade Jr., H.E. Stanley, Tracer dispersion in correlated percolation porous media, *Phys. Rev. E* 61 (2000) 583–587.
- [38] S.V. Patankar, *Numerical Heat Transfer and Fluid Flow*, Hemisphere, Washington DC, 1980.
- [39] J.S. Andrade Jr., D.A. Street, Y. Shibusa, S. Havlin, H.E. Stanley, Diffusion and reaction in percolating pore networks, *Phys. Phys. Rev. E* 55 (1997) 772.
- [40] S. Russ, B. Sapoval, Anomalous viscous damping of vibrations of fractal percolation clusters, *Phys. Rev. Lett.* 73 (1994) 1570.